Since January 2020 Elsevier has created a COVID-19 resource centre with free information in English and Mandarin on the novel coronavirus COVID-19. The COVID-19 resource centre is hosted on Elsevier Connect, the company's public news and information website.

Mathematical Biosciences 325 (2020) 108378

Contents lists available at ScienceDirect

Mathematical Biosciences

journal homepage: www.elsevier.com/locate/mbs

Original research article

Modeling the impact of mass influenza vaccination and public health interventions on COVID-19 epidemics with limited detection capability

Qian Li [a,b], Biao Tang [b], Nicola Luigi Bragazzi [b], Yanni Xiao [a], Jianhong Wu [b,*]

[a] Department of Applied Mathematics, Xi'an Jiaotong University, Xi'an 710049, PR China
[b] Laboratory for Industrial and Applied Mathematics, Department of Mathematics and Statistics, York University, Toronto, Ontario, Canada

ARTICLE INFO

Keywords:
Coronavirus
Pandemic outbreak
Limited resources
Influenza season
Influenza vaccination

ABSTRACT

The emerging coronavirus SARS-CoV-2 has caused a COVID-19 pandemic. SARS-CoV-2 causes a generally mild, but sometimes severe and even life-threatening infection, known as COVID-19. Currently, there exist no effective vaccines or drugs and, as such, global public authorities have so far relied upon non pharmaceutical interventions (NPIs). Since COVID-19 symptoms are aspecific and may resemble a common cold, if it should come back with a seasonal pattern and coincide with the influenza season, this would be particularly challenging, overwhelming and straining the healthcare systems, particularly in resource-limited contexts, and would increase the likelihood of nosocomial transmission. In the present study, we devised a mathematical model focusing on the treatment of people complaining of influenza-like-illness (ILI) symptoms, potentially at risk of contracting COVID-19 or other emerging/re-emerging respiratory infectious agents during their admission at the health-care setting, who will occupy the detection kits causing a severe shortage of testing resources. The model is used to assess the effect of mass influenza vaccination on the spread of COVID-19 and other respiratory pathogens in the case of a coincidence of the outbreak with the influenza season. Here, we show that increasing influenza vaccine uptake or enhancing the public health interventions would facilitate the management of respiratory outbreaks coinciding with the peak flu season, especially, compensate the shortage of the detection resources. However, how to increase influenza vaccination coverage rate remains challenging. Public health decision- and policy-makers should adopt evidence-informed strategies to improve influenza vaccine uptake.

1. Introduction

An emerging coronavirus, currently known as "Severe Acute Respiratory Syndrome coronavirus type 2" (SARS-CoV-2) and previously termed as "2019 novel coronavirus" (2019-nCoV), has spread out from its first reported epicenter and quickly become a pandemic [1,2].

SARS-CoV-2 causes a generally mild, but sometimes severe and even life-threatening infection, known as "coronavirus disease" (COVID-19). Currently, there exist no effective vaccines or drugs that can effectively prevent or treat COVID-19 patients. As such, global public authorities have so far relied upon behavioral, non pharmaceutical interventions (NPIs), such as use of masks, social distancing, self-isolation, quarantine and even lock-down of entire territories and communities, to contain or, at least, mitigate the burden of the ongoing pandemic [3–5]. Despite the unprecedented nature of some of these measures, western countries have found it difficult to fully suppress/eradicate the outbreak and have preferred to mitigate it, deciding to opt for a short-period of NPIs, which will be followed by gradual reopening the economy and return to a new normal. Resumption of daily working and social activities is expected to cause further outbreak waves, due to the re-increasing of contact rates.

In [6], Sajadi et al. provided the evidence that COVID-19 could perhaps prevail at low levels and begin to rise again in late fall and winter in temperate regions in the upcoming year. Since COVID-19 symptoms are aspecific and may resemble a common cold, if it should come back with a seasonal pattern and coincide with the influenza season, this would be particularly challenging. From a clinical standpoint, it would be difficult to distinguish between the two infectious agents, with the definition of COVID-19 cases rather problematic. Moreover, diagnostic tests as well as human resources are limited. Furthermore, currently commercially available rapid diagnostic tests are characterized by a good specificity but have a limited sensitivity, as such not enabling a quick and reliable diagnosis of COVID-19. Altogether, this would significantly impact downstream public health efforts to properly identify COVID-19 cases and contain the outbreak, overwhelming and straining the healthcare systems, particularly in resource-limited contexts, and would increase the likelihood of nosocomial transmission.

* Corresponding author.
E-mail address: wujh@yorku.ca (J. Wu).

https://doi.org/10.1016/j.mbs.2020.108378

Available online 16 May 2020

When the "Severe Acute Respiratory Syndrome" (SARS) outbreak caused by the coronavirus SARS-CoV-1 occurred in mainland China in 2002, the World Health Organization (WHO) has recommended to increase influenza vaccination, considering that the actual coverage rate is still sub-optimal and below the threshold. In particular, the WHO recommended a campaign targeting high-risk groups, such as healthcare workers, the elderly and disabled people, to be able to differentiate more quickly between the two infections and to be more effective in counteracting the outbreak [7–9].

A similar strategy would be valuable also for COVID-19. To test such a hypothesis, we devised a mathematical model incorporating the treatment of people complaining of ILI symptoms, potentially at risk of contracting COVID-19 or other emerging/re-emerging respiratory infectious agents during their admission at the health-care setting, where the competition of the detection resources between the COVID-19 infected population and individuals with ILI symptoms is considered. The main purpose of this study is using the model to assess the effect of mass influenza vaccination and public health interventions on the spread of COVID-19 in the case of a coincidence of the outbreak with the influenza season.

2. Methodology

2.1. Data

We obtained the data of COVID-19 cases in China from January 23rd to March 29th 2020 from the National Health Commission of the People's Republic of China [10]. The data information includes the cumulative number of confirmed cases, the cumulative number of death cases, the cumulative number of cured cases, and the cumulative number of suspected cases, shown in Fig. 1. It should be mentioned that the number of suspected cases includes the number of quarantined COVID-19 exposed cases, the number of quarantined COVID-19 infected cases but not confirmed yet, and the number of quarantined individuals with clinical fever symptoms who are susceptible to COVID-19.

2.2. Model

Based on the epidemical progression of COVID-19 and the intervention measures, we extended the classical SEIR model by including social distancing measures and including "cross-infected" individuals, those who are having clinical fever symptoms and are considered as COVID-19 suspected (and thus quarantined) due to their exposure to COVID-19 infected individuals. The transmission diagram is shown in Fig. 2. In the model, we divide the total population N into ten compartments: susceptible (S), exposed (E), symptomatic infected (I), asymptomatic infected (A), quarantined susceptible (S_q), quarantined susceptible with fever symptoms (S_f), quarantined exposed (E_q), quarantined infected (I_q), confirmed and hospitalized (H), and recovered (R).

With the implementation of contact tracing, a proportion of q of individuals exposed to the virus is quarantined. Let the transmission probability be β and the contact rate be c, then the quarantined individuals can move to compartment E_q (or S_q) at a rate of βcq (or $(1-\beta)cq$) if they are effectively infected (or not effectively infected). While the other proportion, $1-q$, missed from the contact tracing, will move to the exposed compartment E at a rate of $\beta c(1-q)$ once effectively infected or stay in the susceptible compartment S otherwise.

Note that, due to clinical fever or illness-like symptoms, susceptible individuals may also be quarantined and move to the compartment S_f at a transition rate of m, and they can be infected by the quarantined infected individuals at a rate of $\beta_f c_f$. Based on the above assumptions and previous studies [5,11,12], the transmission dynamics is governed by the following model:

$$\begin{cases} S' &= -\frac{(\beta c(t)+c(t)q(t)(1-\beta))SI}{N} - \frac{\beta_A c(t)SA}{N} - m(t)S + \lambda S_q + \lambda_f S_f, \\ E' &= \frac{\beta c(t)(1-q(t))SI}{N} + \frac{\beta_A c(t)SA}{N} - \sigma E, \\ I' &= \sigma\rho E - F_1\left(I, I_q, S_f\right) - \alpha(t)I, \\ A' &= \sigma(1-\rho)E - \gamma_A A, \\ S_q' &= \frac{c(t)q(t)(1-\beta)SI}{N} - \lambda S_q, \\ S_f' &= m(t)S - \beta_f c_f S_f I_q - \lambda_f S_f, \\ E_q' &= \frac{\beta c(t)q(t)SI}{N} + \beta_f c_f S_f I_q - \sigma_q E_q, \\ I_q' &= \sigma_q E_q - F_2\left(I, I_q, S_f\right) - \alpha(t)I_q, \\ H' &= F_1\left(I, I_q, S_f\right) + F_2\left(I, I_q, S_f\right) - \alpha(t)H - \gamma_H(t)H, \\ R' &= \gamma_A A + \gamma_H(t)H. \end{cases} \tag{1}$$

The detailed definitions of all the parameters and variables are listed in Table 1.

A significant difference between the COVID-19 transmission dynamics model in our previous studies [11,12,14] and the current study is the introduction of two saturated functions

$$F_1\left(I, I_q, S_f\right) = \frac{\delta_I I}{1+\omega(t)\left(I+I_q+S_f\right)}$$

and

$$F_2\left(I, I_q, S_f\right) = \frac{\delta_q I_q}{1+\omega(t)\left(I+I_q+S_f\right)},$$

to describe the impact of "cross-infection" on the diagnose rate of the infected class (I) and the detection rate of the quarantined infected class (I_q) with limited testing capacity, respectively. δ_I and δ_q are the fastest diagnose rate of infected individuals and quarantined infected individuals, respectively, that the medical resources permit, $\frac{1}{\omega(t)}$ is the maximum number of individuals who can be tested per unit time (day) (limited by the maximum testing kits and staff to administrate the test) with $\lim_{I\to\infty} F_1\left(I, I_q, S_f\right) = \frac{\delta_I}{\omega(t)}$ and $\lim_{I_q\to\infty} F_2\left(I, I_q, S_f\right) = \frac{\delta_q}{\omega(t)}$. In other word, $\frac{1}{\omega(t)}$ measures the testing capacity per day. Here, we set the daily capacity as an increasing function of time t because of the increasing production of detection kits and the improvement of detection techniques. The function of $\frac{1}{\omega(t)}$ is of the following form:

$$\frac{1}{\omega(t)} = \left(\frac{1}{\omega_0} - \frac{1}{\omega_b}\right)e^{-r_\omega t} + \frac{1}{\omega_b},$$

where $\frac{1}{\omega_0}$ is the total number of available detection kits at the initial time (i.e. January 23^{rd}) with $\omega(0) = \omega_0$, $\frac{1}{\omega_b}$ is the maximum number of available tests permitted with $\lim_{t\to\infty}\omega(t) = \omega_b > \omega_0$, and r_ω is the exponential increasing rate.

The saturation functions $F_1\left(I, I_q, S_f\right)$ and $F_2\left(I, I_q, S_f\right)$ are decreasing functions with respect to S_f. This is because the quarantined COVID-19 susceptible individuals with fever symptoms belong to the COVID-19 suspected population, and will be tested to confirm if they are COVID-19 positive or not. These individuals will consume the detection kits and require staff time, resulting in a slower detection rate of the COVID-19 infected cases.

Similarly to the previous studies [12,14], as a result of the improvement of medical treatment and the implementation of a series of strict control interventions adopted by the Chinese government since January 23rd, we assume that the contact rate c, the quarantine rate q, the quarantine rate of susceptible population with clinical fever symptoms m, disease-induced death rate α, and recovery rate of confirmed individuals γ_H are time-dependent functions. In more details, the contact rate $c(t)$ is a decreasing function with respect to time t, which is given by

$$c(t) = \left(c_0 - c_b\right)e^{-r_c t} + c_b,$$

where c_0 is the contact rate at the initial time with $c(0) = c_0$, c_b is the minimum contact rate under control measures and self-isolation with $\lim_{t\to\infty} c(t) = c_b < c_0$, and r_c is the exponential decreasing rate.

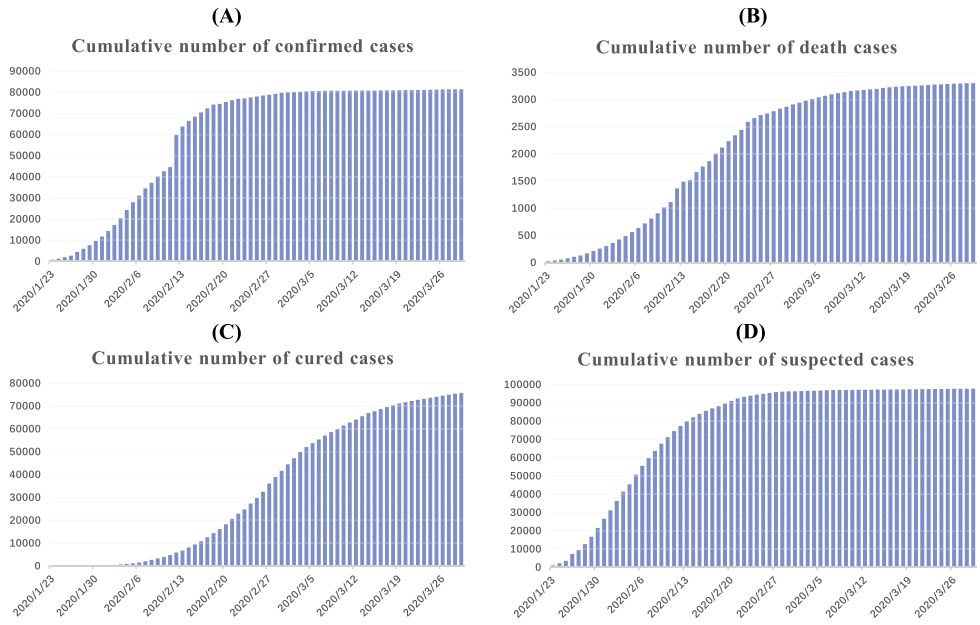

Fig. 1. The data of COVID-19 in China from January to March 2020. (A) The cumulative number of confirmed cases; (B) The cumulative number of death cases; (C) The cumulative number of cured cases; (D) The cumulative number of suspected cases.

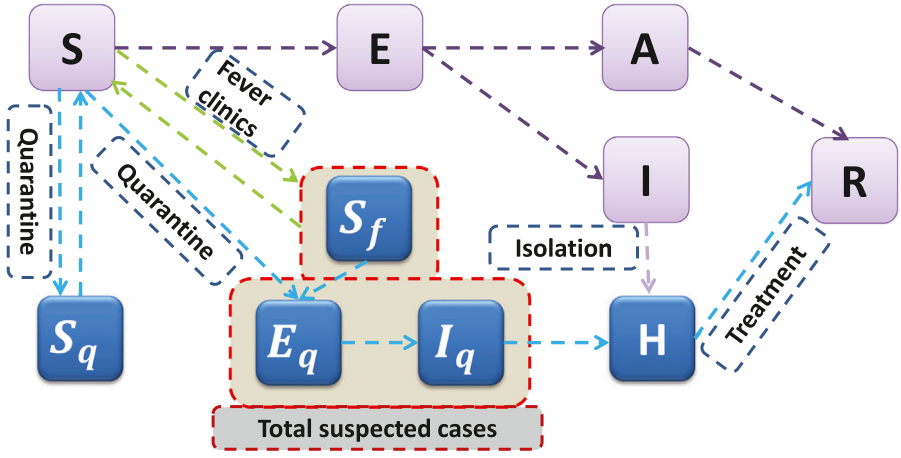

Fig. 2. Diagram of the model adopted in the study for illustrating the COVID-19 infection dynamics. Interventions including intensive contact tracing followed by quarantine and isolation are indicated. The total suspected cases consisting of quarantined susceptible with clinical fever symptoms (S_f), quarantined exposed (E_q), and quarantined infected (I_q).

The quarantined rate q is an increasing function with respect to time t due to the strengthened contact tracing, which takes the following form

$$q(t) = \left(q_0 - q_b\right) e^{-r_q t} + q_b,$$

where q_b is the quarantined rate at the initial time with $q(0) = q_0$, q_b is the maximum quarantined rate under control measures with $\lim_{t\to\infty} q(t) = q_b > q_0$, and r_q is the exponential increasing rate.

The quarantined rate of susceptible population with clinical fever symptoms $m(t)$ is a decreasing function with respect to time t, given by

$$m(t) = \left(m_0 - m_b\right) e^{-r_m t} + m_b,$$

where m_0 denotes the quarantined rate of susceptible population with fever symptoms at the initial time with $m(0) = m_0$, m_b is the minimum quarantined rate of susceptible population with fever symptoms with $\lim_{t\to\infty} m(t) = m_b < m_0$, and r_m is the exponential decreasing rate.

Due to the improvements of medical treatments and the strengthening of the production and supply of prevention and control products [15], disease-induced death rate $\alpha(t)$ decreases with respect to time t, and the recovery rate of confirmed individuals $\gamma_H(t)$ increases with respect to time t. Thus $\alpha(t)$ and $\gamma_H(t)$ take the following forms,

$$\alpha(t) = \left(\alpha_0 - \alpha_b\right) e^{-r_\alpha t} + \alpha_b, \quad \text{and} \quad \gamma_H(t) = \left(\gamma_{H0} - \gamma_{Hb}\right) e^{-r_\gamma t} + \gamma_{Hb},$$

where α_0 is the disease-induced death rate at the initial time with $\alpha(0) = \alpha_0$, α_b is the minimum disease-induced death rate with $\lim_{t\to\infty} \alpha(t) = \alpha_b < \alpha_0$, and r_α is the exponential decreasing rate. γ_{H0} denotes the recovery rate of confirmed individuals at the initial time with $\gamma_H(0) = \gamma_{H0}$, γ_{Hb} denotes the maximum recovery rate of confirmed individuals with $\lim_{t\to\infty} \gamma_H(t) = \gamma_{Hb} > \gamma_{H0}$, and r_γ denotes the exponential increasing rate.

Using the next generation matrix, we can define and calculate the effective reproduction number R_t as follows:

$$R_t = max\left\{R_1(t), R_2(t)\right\},$$

where

$$R_1(t) = \frac{\rho\beta c(t)(1-q(t))S_t}{\left(\alpha(t) + \delta_I / \left(1 + \omega(t)S_{ft}\right)\right) N} + \frac{(1-\rho)\beta_A c(t) S_t}{\gamma_A N},$$

Table 1
Parameter estimates for the COVID-19 epidemics in China.

Parameter		Definition	Value	Source
	c_0	Contact rate at the initial time	14.781	[11]
$c(t)$	c_b	Minimum contact rate with control strategies	2.0	Estimated
	r_c	Exponential decreasing rate of contact rate	0.1	Estimated
β		Transmission probability from I to S per contact	0.18	Estimated
	q_0	Quarantined rate at the initial time	1.0×10^{-4}	[12]
$q(t)$	q_b	Maximum quarantined rate with control strategies	0.9	Estimated
	r_q	Exponential increasing rate of quarantined rate	0.1	Estimated
β_A		Transmission probability from A to S per contact	0.01	Estimated
	m_0	Quarantined rate of susceptible population with fever symptoms at the initial time	2.0848×10^{-4}	Estimated
$m(t)$	m_b	Minimal quarantined rate of susceptibles with fever symptoms	5.0001×10^{-7}	Estimated
	r_m	Exponential decreasing rate of quarantined rate	0.0567	Estimated
λ		Releasing rate of quarantined susceptibles	1/14	[11]
λ_f		Releasing rate of quarantined susceptibles with fever symptoms	0.1	Estimated
ρ		Ratio of symptomatic infection	0.5	Estimated
σ		Transition rate of exposed individuals to the infected class	1/5	[13]
δ_I		Fast diagnose rate of infected individuals	0.5	Estimated
	$1/\omega_0$	Initial number of detection kits per day	2000	Estimated
$1/\omega(t)$	$1/\omega_b$	Maximal number of detection kits per day	1.0×10^{-5}	Estimated
	r_ω	Exponential increasing rate of the number of detection kits	0.885	Estimated
γ_A		Recovery rate of asymptotic infected individuals	0.13978	[11]
	α_0	Disease-induced death rate at the initial time	0.012	Estimated
$\alpha(t)$	α_b	Minimal disease-induced death rate with treatment	0.0012	Estimated
	r_α	Exponential increasing rate of disease-induced death rate	0.1129	Estimated
β_f		Transmission rate from I_q to S_f	3.0×10^{-6}	Estimated
c_f		Contact rate of suspected cases	2.0	Estimated
σ_q		Transition rate of quarantined exposed individuals to the quarantined infected class	0.2	Estimated
δ_q		Fast diagnose rate of quarantined individuals	1.0	Estimated
	γ_{H0}	Recovery rate of confirmed individuals at the initial time	0.001	Estimated
$\gamma_H(t)$	γ_{Hb}	Maximal recovery rate of confirmed individuals with treatment	0.15	Estimated
	r_γ	Exponential increasing rate of recovery rate	0.0123	Estimated

Variable	Definition	Initial value	Source
S	Susceptible population	1.5×10^7	Estimated
E	Exposed population	8216	Estimated
I	Infected symptomatic population	1000	Estimated
A	Infected asymptomatic population	1000	Estimated
S_q	Quarantined susceptible population	7347	Data
S_f	Quarantined susceptible population with fever symptoms	499.9975	Estimated
E_q	Quarantined exposed population	100.0003	Estimated
I_q	Quarantined infected population	250.0005	Estimated
H	Confirmed and hospitalized population	771	Data
R	Recovered population	34	Data

and

$$R_2(t)=\frac{\beta_f c_f S_{ft}}{\left(\alpha(t)+\delta_q/\left(1+\omega(t)S_{ft}\right)\right)} \text{ with } S_t=S(t) \text{ and } S_{ft}=S_f(t).$$

Note that $R_2(t)$ represents the effective reproduction number of cross-infected individuals.

3. Main results

3.1. Parameter estimation process

In order to fit the model to the data, we firstly fix some parameters of our model from previous literature to reduce the complexity. In particular, the contact rate and the quarantined rate at the initial time are fixed as $c_0=14.781$ [11] and $q_0=1.0\times10^{-4}$ [12], respectively. The incubation period is fixed as 5 days [13], i.e. $\sigma=1/5$, the releasing rate of quarantined susceptible individuals is fixed as $\lambda=1/14$ [11], while the recovery rate of the asymptomatic infected individuals is fixed as $\gamma_A=0.13978$ [11]. In addition, we fix the initial quarantined susceptible population, confirmed and hospitalized population, and recovered population as 7374, 771 and 34 respectively according to the data information.

By simultaneously fitting the proposed model to the cumulative number of confirmed cases, cumulative number of death cases, cumulative number of cured cases and cumulative number of suspected cases, we first estimate the rest parameters and initial conditions using the least square method. The best fitting curves are marked as red in Fig. 3 with the blue circles representing the data from January 23rd to March 29th 2020. The detailed estimated values of the parameters and initial conditions are listed in Table 1.

It is worth mentioning that we use four time series of data to fit the model, simultaneously, which can cross-validate the estimation results. Furthermore, based on the available information, the least squares method with a *priori* distribution for each parameter is used in this study. In another word, we implicitly utilize a penalized least square method to select reasonable parameter values falling in the ranges which were estimated in other published studies. Particularly, our estimated minimum contact rate with control strategies is 2.0 which is consistent with contact surveys in study [16], and the transition rate

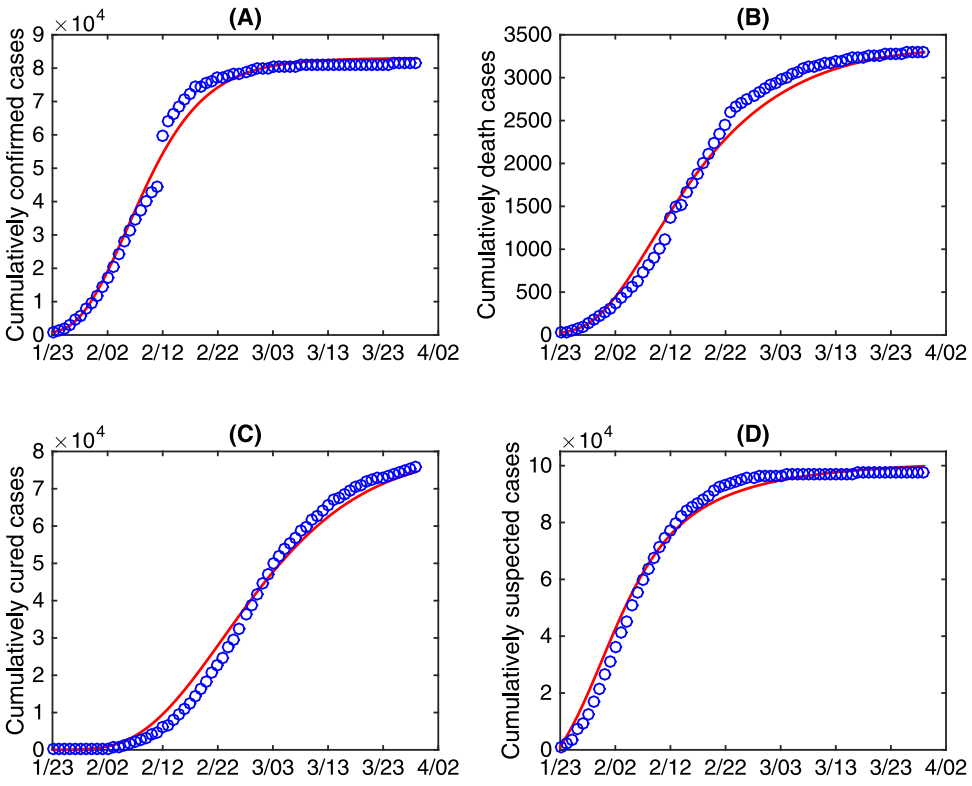

Fig. 3. Best model fitting result. The red curves are the best fitting curves, and the blue circles denote the cumulatively confirmed cases, cumulatively death cases, cumulatively cured cases and cumulatively suspected cases.

of quarantined exposed individuals to the quarantined infected class is estimated as $\sigma_q = 0.2$ being in line with the incubation period [13]. It was illustrated in [17] that it takes about 2 days from the start of sampling to the return of results, indicating that our estimation value of fast diagnose rate of infected individuals $\delta_I = 0.5$ is reasonable. Furthermore, the estimated initial number of detection kits per day $1/\omega_0 = 2000$ is highly consistent with the news reported in the Beijing News [17].

Furthermore, we use the coefficient of determination (R^2) to estimate the goodness of fit for our model fitting results. Given a data set with n observed value $y_1, \ldots, y_n$. The corresponding estimated values from the model are defined as $f_1, \ldots, f_n$ and $\bar{y} = \frac{1}{n}\sum_{i=1}^{n} y_i$ is the average observed value, then the coefficient of determination value (R_2) can be defined as $R^2 = 1 - \frac{SS_{res}}{SS_{tot}}$ with $SS_{res} = \sum_{i=1}^{n}\left(y_i - f_i\right)^2$ denoting the sum of squares of residuals and $SS_{tot} = \sum_{i=1}^{n}\left(y_i - \bar{y}\right)^2$ denoting the total sum of squares. Therefore, we obtain the coefficients of determination for the model fitting results in Fig. 3(A-D) being 0.9905, 0.988, 0.9884 and 0.9868, respectively. This indicates that the model fits the data very well.

3.2. Impacts of limited detection kits

Detection kits for COVID-19 were firstly introduced and used on January 16th 2020, but with very limited number. Since January 23rd 2020, detection kits were delivered to Hubei province from other provinces in China. Since it took time to increase the production of kits and improve the level of production technology, there was a serious shortage of detection kits during the initial stage of the COVID-19 epidemics. To examine the impacts of the limited detection kits on the COVID-19 epidemics in terms of the cumulative number of confirmed cases, the cumulative number of cross-infected cases and the infected population ($I(t)$), we vary the increasing rate of the available detection kits r_ω in Fig. 4. It follows from Fig. 4 that reducing r_ω will significantly increase both the cumulative number of confirmed cases and cross-infected cases, and the infected population of $I(t)$ and daily cross-infected population at the peak time. Particularly, the cumulatively confirmed cases and cumulatively cross-infected cases will increase 3.5 times (about 2.084×10^5 cases) and 4.7 times (about 1.483×10^4 cases), respectively, if the exponential increasing rate r_ω decreases by 80 percent. This means that deficiency and delay of detection cause more serious outbreaks. In another word, speeding up the production of detection kits and improve the detection capability play an important role in reducing the final size of infections.

When faced with limited detection kits supply, we show the impacts of public health interventions on the outbreak of COVID-19, as seen in Table 2. In particular, increasing r_c or r_q remarkably reduces the cumulative number of confirmed cases. Specifically, when r_ω is very small ($r_\omega = 0.1 \times r_\omega^0$), i.e. the testing kits production increases very slowly, then (1). If r_c increases by 5 times, the cumulative number of confirmed cases will decrease by 93.6%; (2). If r_q increases by 5 times, the cumulative number of confirmed cases will decrease by 78.7%. In addition, comparing the results in Table 2, we find that the impact of increasing r_c or r_q on mitigating the epidemics weakens as r_ω increases. This implies that rapid implementation of public health interventions, such as reducing contact rate and enhancing quarantined rate, is a good way to compensate the shortage of detection kits, and it is more indispensable for countries with severe limited resource of detection kits.

It is also interesting to observe from Fig. 5(A) that the estimated effective reproduction number (the blue curve) will first experience a short-period increasing before it decreases below the threshold 1. However, we further observe that if we increase the rate of r_ω by 5 times (the red curve in Fig. 5(A)), the effective reproduction number will decrease below the threshold 1 directly. This indicates that due to the limited resource of the testing kits, the fast-increased infected population will result in more infections as they are not confirmed and hospitalized. And the situation will become worse if r_ω is smaller, shown in Fig. 5(A) as well. Furthermore, it follows from Fig. 5(B) and (C) that increasing r_c or r_q can avoid the magnification of the effective reproduction number and make the threshold value reduce to

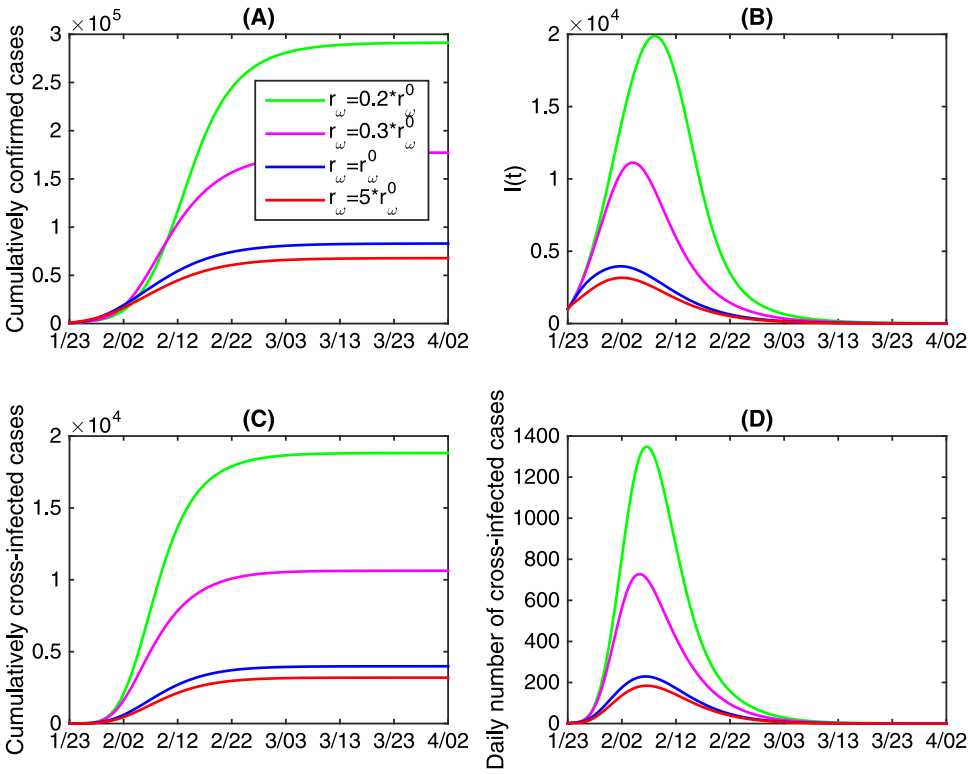

Fig. 4. The effects of varying the increasing rate of available detection kits r_ω on the COVID-19 epidemic in mainland China. r_ω^0 denotes the estimated value of r_ω.

Table 2
The impacts of public health interventions on the cumulative number of confirmed cases when faced with limited detection kits supply.

Value of r_ω	Cumulative number of confirmed cases with varying r_c			Cumulative number of confirmed cases with varying r_q		
	$r_c = r_c^0$	$r_c = 2 * r_c^0$	$r_c = 5 * r_c^0$	$r_q = r_q^0$	$r_q = 2 * r_q^0$	$r_q = 5 * r_q^0$
$r_\omega = 0.1 * r_\omega^0$	9.564×10^5	1.859×10^5 (−80.6%)	6.087×10^4 (−93.6%)	9.564×10^5	3.981×10^5 (−58.4%)	2.035×10^5 (−78.7%)
$r_\omega = 0.4 * r_\omega^0$	1.357×10^5	5.910×10^4 (−56.4%)	2.649×10^4 (−80.5%)	1.357×10^5	1.045×10^5 (−23.0%)	7.759×10^4 (−42.8%)
$r_\omega = 0.7 * r_\omega^0$	9.510×10^4	4.539×10^4 (−52.3%)	2.223×10^4 (−76.6%)	9.510×10^4	7.685×10^4 (−19.2%)	6.003×10^4 (−36.9%)
$r_\omega = r_\omega^0$	8.302×10^4	4.069×10^4 (−51.0%)	2.070×10^4 (−75.1%)	8.302×10^4	6.80×10^4 (−18.1%)	5.40×10^4 (−35.0%)

Note that r_ω^0, r_c^0 and r_q^0 are the estimated value of r_ω, r_c and r_q, respectively.

1 ahead of time, which implies that reducing the contact rate quickly and increasing the quarantined rate can effectively avert the short-term intensification of the outbreak caused by the limited detection kits.

3.3. Benefits of getting vaccinated against influenza

The COVID-19 outbreak in China coincided partially with flu season, and it was difficult to distinguish COVID-19 accurately and rapidly from influenza-like-illnesses. As a result, individuals with clinical fever symptoms required medical treatment in high risk settings of COVID-19, and the risk of cross-infection increased. Here we seek to use our transmission dynamics model to explore the impact of mass influenza vaccination prior to the onset of flu season on controlling the transmission of COVID-19.

Note that, in our model, we assumed that due to the influenza-like-illness (ILI), the susceptible individuals (S) can be quarantined at a rate of m (move to S_f), which is proportion to the susceptible population. Further, we assume that the susceptible population is vaccinated against influenza with an effective vaccination coverage rate Vr. Thus, the vaccinated population will not be quarantined because of the clinical fever symptoms, consequently, the rate at which the susceptible population is quarantined due to the ILI becomes $(1-Vr) * m * S$. Based on the above assumptions, we evaluate the impact of the mass influenza vaccination on the transmission dynamics of COVID-19.

In Fig. 6, by changing the vaccination coverage rate of Vr and fixing all the other parameters as the estimated baseline values, we examine the impact of vaccination against influenza on the COVID-19 epidemics in China in terms of the final size and the peak values. It follows from Fig. 6 that increasing the vaccination coverage rate against influenza can remarkably reduce the cumulative number of COVID-19 confirmed cases and cross-infected cases, and also reduce the peak number of $I(t)$ and daily cross-infected population. In more detail, we find that by a vaccination coverage rate of 90%, the cumulative number of confirmed cases can reduce by 23.0% (about 19062 total cases), moreover, the cumulative number of cross-infected cases can reduce by 92.9% (about 3700 cases). This implies that mass influenza vaccination could contribute significantly to the control of the outbreak of COVID-19 and significantly reduce the risk of cross-infection.

In addition, in Fig. 7 we illustrate the impact of getting vaccine against influenza on the reduction of the cumulative number of confirmed cases and cross-infected cases incorporating the effect of limited testing kits and public health interventions, that is, with different

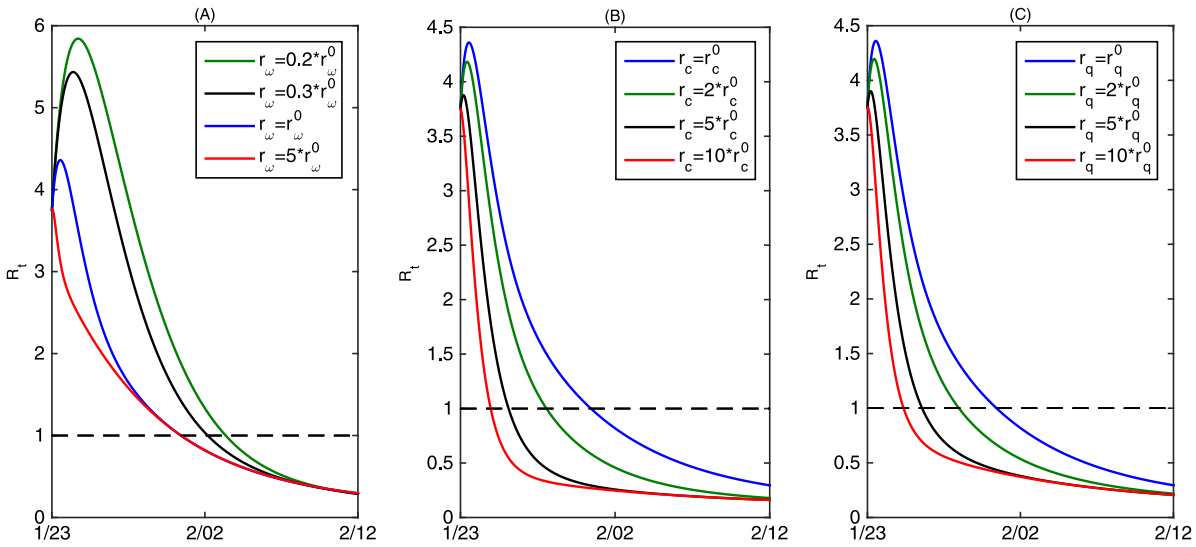

Fig. 5. (A) Estimated effective reproduction number (blue curve) and the variation of the effective reproduction number by varying r_ω; (B) The variation of the effective reproduction number by varying r_c; (C) The variation of the effective reproduction number by varying r_q. Here r_ω^0 denotes the estimated value of the increasing rate of available detection kits r_ω, r_c^0 denotes the estimated value of the decreasing rate of contact rate r_c, and r_q^0 denotes the estimated value of the increasing rate of quarantined rate r_q.

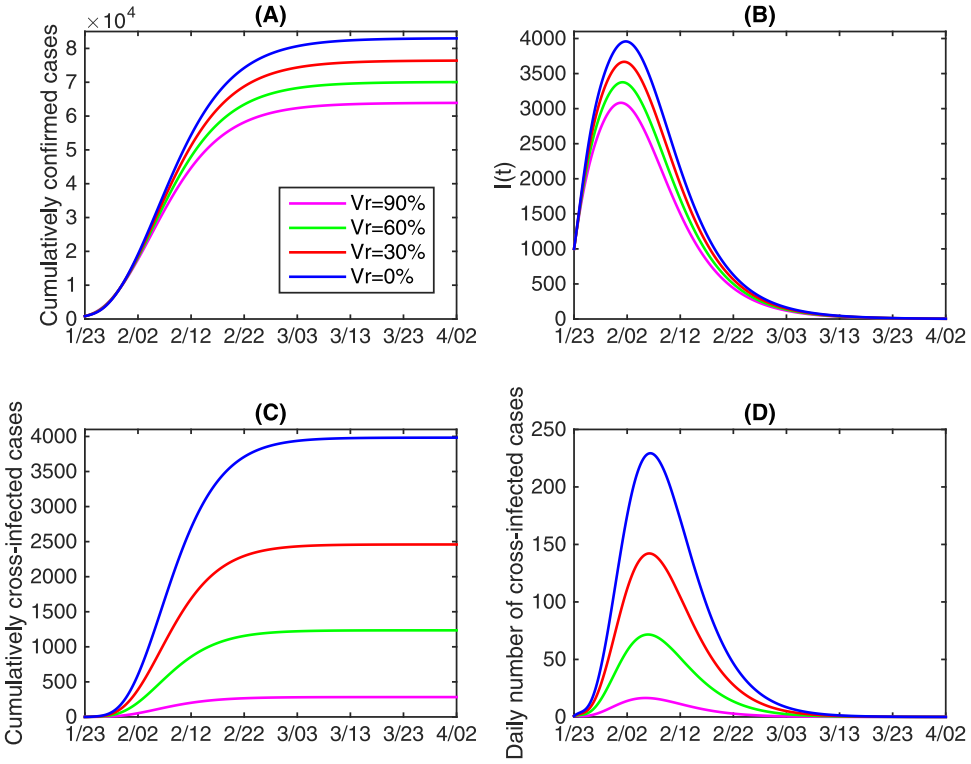

Fig. 6. The impacts of getting vaccinated against influenza on the COVID-19 epidemic in mainland China. Here "Vr" represents the vaccination coverage rate against influenza.

increasing rate of available detection kits r_ω or different decreasing rate of contact rate r_c. As shown in Fig. 6, vaccination against influenza could reduce the cumulative numbers of confirmed cases and cumulative cross-infected cases, hereafter referred as the reduced confirmed cases and reduced cross-infected cases, respectively. It follows from Fig. 7(A_1) and (A_2) that getting vaccinated against influenza could significantly reduce the cumulative number of confirmed cases and cross-infected cases with respect to r_ω. We give the specific reduction rate with respect to different r_ω and vaccination coverage rate in Table 3. Specifically, when the vaccination coverage rate was 90%, the cumulative number of confirmed cases and cross-infected cases could reduce by 51.5% and 91.4% with $r_\omega = 0.1 \times r_\omega^0$, respectively. We can further observe that the effects of getting vaccinated against influenza weakens as r_ω increases. It means that getting vaccinated against influenza could effectively control the outbreak of COVID-19. Moreover, mass influenza vaccination is more necessary when detection kits are severely limited and under seriously shortage of supply. In another words, mass influenza vaccination can be a much more effective control measure in mitigating the COVID-19 epidemics in the early stage with a rapid growth and the countries or areas with limited testing kits.

Similarly, Fig. 7(B_1) and (B_2) illustrate the impact of getting vaccinated on reducing the cumulative number of confirmed cases and cross-infected cases with respect to r_c, and the detailed reduction rate with respect to different r_c and vaccination coverage rate is given

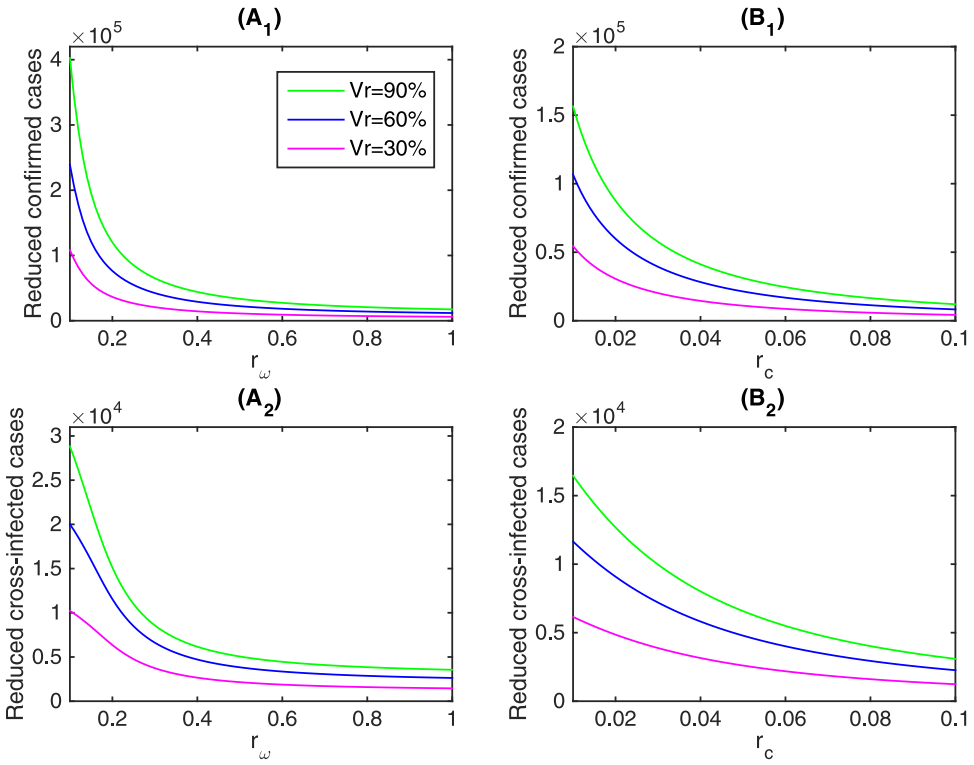

Fig. 7. The total reduction number of cumulatively confirmed cases and the reduction of cumulatively cross-infected cases by different vaccination coverage rate against influenza with respect to r_ω (A_1 and A_2) and r_c (B_1 and B_2). Here "Vr" represents the vaccination coverage rate against influenza.

Table 3
The impacts of getting vaccinated against influenza on the cumulative number of confirmed cases and the cumulative number of cross-infected cases with respect to r_ω.

Vaccination coverage rate	Cumulative number of confirmed cases			Cumulative number of cross-infected cases		
	$r_\omega = 0.1 * r_\omega^0$	$r_\omega = 0.4 * r_\omega^0$	$r_\omega = 0.7 * r_\omega^0$	$r_\omega = 0.1 * r_\omega^0$	$r_\omega = 0.4 * r_\omega^0$	$r_\omega = 0.7 * r_\omega^0$
0	9.564×10^5	1.357×10^5	9.510×10^4	3.295×10^4	7.427×10^3	4.681×10^3
30%	8.273×10^5 (−13.5%)	1.189×10^5 (−12.4%)	8.616×10^4 (−9.4%)	2.245×10^4 (−31.9%)	4.380×10^3 (−41.0%)	2.844×10^3 (−39.2%)
60%	6.684×10^5 (−30.1%)	1.017×10^5 (−25.1%)	7.735×10^4 (−18.7%)	1.226×10^4 (−62.8%)	2.035×10^3 (−72.6%)	1.395×10^3 (−70.2%)
90%	4.635×10^5 (−51.5%)	8.386×10^4 (−38.2%)	6.860×10^4 (−27.9%)	2.830×10^3 (−91.4%)	410.8 (−94.5%)	309.2 (−93.4%)

Here r_ω^0 is the estimated value of r_ω.

Table 4
The impacts of getting vaccinated against influenza on the cumulative number of confirmed cases and the cumulative number of cross-infected cases with respect to r_c.

Vaccination coverage rate	Cumulative number of confirmed cases			Cumulative number of cross-infected cases		
	$r_c = 0.1 * r_c^0$	$r_c = 0.5 * r_c^0$	$r_c = r_c^0$	$r_c = 0.1 * r_c^0$	$r_c = 0.5 * r_c^0$	$r_c = r_c^0$
0	7.907×10^5	1.798×10^5	8.302×10^4	2.013×10^4	8.363×10^3	3.983×10^3
30%	7.062×10^5 (−10.7%)	1.632×10^5 (−9.2%)	7.644×10^4 (−7.9%)	1.314×10^4 (−34.7%)	5.222×10^3 (−37.6%)	2.460×10^3 (−38.2%)
60%	6.249×10^5 (−21.0%)	1.472×10^5 (−18.1%)	7.010×10^4 (−15.6%)	6.927×10^3 (−65.6%)	2.641×10^3 (−68.4%)	1.235×10^3 (−69.0%)
90%	5.468×10^5 (−30.8%)	1.317×10^5 (−26.8%)	6.393×10^4 (−23.0%)	1.616×10^3 (−92.0%)	601.2 (−92.8%)	283.0 (−92.9%)

Here r_c^0 is the estimated value of r_c.

in Table 4. Specifically, for a 90% vaccination coverage rate, the cumulative number of confirmed cases could reduce by 30.8%, and the cumulative number of cross-infected cases could reduce by 92.0% with $r_c = 0.1 \times r_c^0$, showing that if the contact rate was not fast controlled and reduced, mass vaccination could effectively aid the containment of COVID-19 outbreak.

4. Discussions and conclusions

In the present mathematical modeling study, we have tested the hypothesis that a mass influenza vaccination campaign would have a positive effect on the management of people with non-specific symptoms and complaining of ILIs, potentially at risk of developing the COVID-19 (or other emerging respiratory infections) during their admission at the health-care setting. Our findings show that increasing influenza vaccination coverage rate to an optimal threshold would facilitate the efforts of containing the COVID-19 outbreak.

According to some researchers, the SARS-CoV-2 had already been circulating much earlier than late December 2019 but its correct identification was hindered by a considerable amount of people complaining of influenza-like-illness (ILI) symptoms. In the case of the implementation of a mass influenza vaccination campaign well before the onset of the influenza season, the exposure of emerging/re-emerging respiratory pathogens would be unmasked, facilitating their identification and the design of ad hoc public health interventions. This would significantly alleviate the pressure on health-care facilities, reducing the total number of people complaining of ILI symptoms, and decreasing the transmission probability of COVID-19 or other emerging infectious agents both among healthcare workers and, subsequently, among people under investigation for their disease.

Influenza generates a relevant burden worldwide, both in terms of healthcare resources consumption and socio-economic impact. Despite the existence of effective vaccines and their importance as cost-effective preventative tool, vaccination coverage rate still remains suboptimal. With respect to the general population, healthcare workers are at a higher risk of exposure to circulating respiratory pathogens, including influenza, potentially threatening their own health and compromising patients' safety. Influenza vaccine uptake is suboptimal also among other targeted categories, including the elderly and disabled people. An inadequate disease risk perception, a low health literacy, perception of the societal effects of vaccination and alleged side-effects are among the drivers of vaccine hesitancy.

Influenza vaccination would enable to better control and contain the spread of COVID-19 or other emerging/re-emerging pathogens, in case of coincidence of the outbreak with the influenza season. Mass influenza vaccination prior to the onset of the peak influenza season would significantly decrease the number of ILIs among the general population and specifically the elderly, with fewer persons with ILIs seeking for medical advice, particularly those in high-risk settings, with frailty, underlying co-morbidities or disabled. As such, this would minimize the probability of not quickly and accurately identifying circulating respiratory pathogens as well as the possibility of ongoing nosocomial transmission.

However, how to increase influenza vaccination coverage rate remains challenging. Mandatory policies for targeted categories are under debate in several countries. Also, in this study, we did not consider explicitly the efficacy of the influenza vaccine, and the vaccination coverage should be an effective vaccination rate. However, we believe that this study provided a fundamental framework for quantitatively evaluating the impact of vaccination against influenza on mitigating the COVID-19 epidemics. Public health decision- and policy-makers should adopt evidence-informed strategies to improve influenza vaccine uptake, given its impact on respiratory pandemic outbreaks coinciding with the peak influenza season and the shortage of medical personnel and equipment, including diagnostic tests.

Declaration of competing interest

The authors declare that they have no known competing financial interests or personal relationships that could have appeared to influence the work reported in this paper.

Acknowledgments

YX was supported by the National Natural Science Foundation of China (NSFC, 11631012), JW was supported by the Canadian Institute of Health Research (CIHR) 2019 Novel Coronavirus (COVID-19) rapid research program.

References

[1] S.M. Kissler, C. Tedijanto, E. Goldstein, Y.H. Grad, M. Lipsitch, Projecting the transmission dynamics of SARS-CoV-2 through the postpandemic period, Science 14 (2020) http://dx.doi.org/10.1126/science.abb5793.

[2] K. Leung, J.T. Wu, D. Liu, G.M. Leung, First-wave COVID-19 transmissibility and severity in China outside Hubei after control measures, and second-wave scenario planning: a modelling impact assessment, Lancet 395 (10233) (2020) 1382–1393.

[3] Q.Y. Lin, S. Zhao, D.Z. Gao, W.M. Wang, L. Yang, D.H. He, A conceptual model for the coronavirus disease 2019 (COVID-19) outbreak in Wuhan, China with individual reaction and governmental action, Int. J. Infect. Dis. (2020) http://dx.doi.org/10.1016/j.ijid.2020.02.058.

[4] E. Shim, A. Tariq, W. Choi, Y. Lee, G. Chowell, Transmission potential and severity of COVID-19 in South Korea, Int. J. Infect. Dis. 93 (2020) 339–344.

[5] C.N. Ngonghala, E. Iboi, S. Eikenberry, M. Scotch, C.R. MacIntyre, M.H. Bonds, A.B. Gumel, Mathematical assessment of the impact of non-pharmaceutical interventions on curtailing the 2019 novel coronavirus, 2020, arXiv preprint arXiv:2004.07391.

[6] M.M. Sajadi, P. Habibzadeh, A. Vintzileos, S. Shokouhi, F. Miralles-Wilhelm, A. Amoroso, Temperature, humidity and latitude analysis to predict potential spread and seasonality for COVID-19, 2020, Available at SSRN: https://ssrn.com/abstract=3550308.

[7] P. Schlagenhauf, Influenza vaccine enlisted to prevent SARS confusion, Lancet 362 (9386) (2003) 809.

[8] G. Dini, A. Toletone, L. Sticchi, A. Orsi, N.L. Bragazzi, P. Durando, Influenza vaccination in healthcare workers: A comprehensive critical appraisal of the literature, Hum. Vaccin Immunother 14 (3) (2018) 772–789, http://dx.doi.org/10.1080/21645515.2017.1348442.

[9] R.E. Thomas, D.L. Lorenzetti, Interventions to increase influenza vaccination rates of those 60 years and older in the community, Cochrane Database Syst. Rev. 5 (2018) CD005188, http://dx.doi.org/10.1002/14651858.

[10] National Health Commission of the People's Republic of China, 2020, http://www.nhc.gov.cn/xcs/yqfkdt/gzbd_index.shtml. (Accessed 5 April 2020).

[11] B. Tang, X. Wang, Q. Li, N.L. Bragazzi, S.Y. Tang, Y.N. Xiao, J.H. Wu, Estimation of the transmission risk of the 2019-nCoV and its implication for public health interventions, J. Clin. Med. 9 (2) (2020) 462, http://dx.doi.org/10.3390/jcm9020462.

[12] B. Tang, F. Xia, S.Y. Tang, N.L. Bragazzi, Q. Li, X.D. Sun, J.H. Liang, Y.N. Xiao, J.H. Wu, The effectiveness of quarantine and isolation determine the trend of the COVID-19 epidemics in the final phase of the current outbreak in China, Int. J. Infect. Dis. (2020) http://dx.doi.org/10.1016/j.ijid.2020.03.018.

[13] Special Expert Group for Control of the Epidemic of Novel Coronavirus Pneumonia of the Chinese Preventive Medicine Association, The Chinese Preventive Medicine Association, An update on the epidemiological characteristics of novel coronavirus pneumonia (COVID-19), Chin. J. Epidemiol. 41 (2020) 139–144.

[14] B. Tang, N.L. Bragazzi, Q. Li, S.Y. Tang, Y.N. Xiao, J.H. Wu, An updated estimation of the risk of transmission of the novel coronavirus (2019-nCov), Infect. Dis. Model. 5 (2020) 248–255.

[15] Hubei Provincial People's Government. http://hubei.gov.cn/zwgk/hbyw/hbywqb/202001/t20200123_2014361.shtml.

[16] J.J. Zhang, M. Litvinova, Y.X. Liang, Y. Wang, W. Wang, S.L. Zhao, Q.H. Wu, S. Merler, C. Viboud, A. Vespignani, M. Ajelli, H.J. Yu, Changes in contact patterns shape the dynamics of the COVID-19 outbreak in China, Science (2020) http://dx.doi.org/10.1126/science.abb8001.

[17] Beijing News. http://www.bjnews.com.cn/news/2020/01/24/679052.html.